Resource Allocation for Maximizing Spectral Efficiency in a Multiuser MFSK System

Manish Sharma and Daniel Basso Ferreira

***Abstract*—In this paper we explore strategies to improve the spectral efficiency values of a multiuser M-ary Frequency Shift Keying (MFSK) system when a fast and frequency selective fading channel with limited bandwidth is available and a fixed number of receiving antennas are present at the base station. Two options are considered: bandwidth partitioning and cell sectoring, where random user distribution and the effects of antenna directivity on signal to noise ratio was considered. Results show that in this situation the best case scenario is the one in which all users share the whole bandwidth instead of partitioning it. Also, given the limitation on available antennas and radio frequency receiver chains at the base station, it is better to divide a cell into as many sectors as possible, even at the cost of losing spatial diversity in each sector. Given the constraints, sectoring allows the system to reach values of spectral and energy efficiencies unachievable by spatial diversity by itself.**

***Index Terms*—Spectral efficiency, multiuser communications, fading channels, diversity.**

I. Introduction

Consider the situation in which U mobile users wish to transmit information to a base station. The available channel suffers fast and frequency selective Rayleigh fading, eliminating the possibility of estimation and tracking of channel's state by the system. The number of available antennas at the base station and system bandwidth W are limited. The objective of this system is to transmit as much data as possible, which is equivalent to having the highest possible spectral efficiency (SE). One possible transmission scheme is to use MFSK modulation [1] and non coherent multiuser detection, which has been shown to increase overall system capacity when compared to single user detection [2].

M. Sharma and D. B. Ferreira are with Aeronautics Institute of Technology (ITA), São José dos Campos, SP, Brazil. E-mails:[manish][danielbf]@ita.br

M. Sharma was partially supported by grant 2013/25977-7, São Paulo Research Foundation (FAPESP)

Digital Object Identifier: 10.14209/jcis.2022.13

Diversity [3], [4], [5] also improves SE in a number of situations, including the one considered. Spatial diversity can be obtained by using multiple antennas. Their signals may be processed in a variety of ways that increase performance. On the other hand, if a fixed number of L antennas may be used, total transmission rate could be improved using directive antennas and dividing the covered region (a cell) into sectors. Sectoring has the advantage of potentially increasing received signal power due to higher antennas' gain and, in this case, reducing the number of users sharing the channel at the same time. Sectoring could be detrimental because randomly distributed users could at times agglomerate in one particular sector (covered by less than L antennas) while other sectors remain idle, potentially reducing efficiency of the system as a whole. The question is to determine in this condition how to employ L antennas to cover a cell that is shared by U users. To the best of our knowledge this question has not been answered before.

This problem falls within the context of fifth generation (5G) and beyond 5G (B5G) communication systems because MFSK [6] and massive MIMO [7] have been considered for ultra wideband channels that suffer fast and frequency selective fading[8], [9]. Highly directive beams, statically or dynamically generated, have the advantage of decreasing Doppler spread [10], increasing coherence time. Even in this case, a short enough coherence time due to high relative speed between transmitter and receiver prevents acquiring and tracking channel state information (CSI) such as in the considered situation. The added complexity and processing delay required for CSI may also be undesired or unfeasible for ultra-reliable low-latency use cases, e.g. vehicular communications. These prohibit massive MIMO strategies that rely on CSI to achieve high SE. Another inherent problem of higher radio frequency communication channels is its relatively higher path loss. Given the same transmission

power constraint, the distance between transmitter and receiver should be shorter, thus increasing the number of required base stations to cover a given area. This, in turn, makes the number of antennas and radio frequency receiver chains at each base station an economically relevant factor. Beamforming [11], [12] could in theory completely separate user signals given a sufficient number of antennas, but it requires additional computational complexity to perform tasks such as direction of arrival and beam pattern estimation that are not needed when statically sectoring. The choice of using diversity or sectoring is not a replacement for distributed antenna systems [13], small cells [14], [15], or power allocation algorithms [16]. Rather, it may be used in conjunction with these methods to further improve system SE.

It is of interest to know which is better: to use diversity or to use sectoring. These two are comparable because there is negligible signal detection complexity difference when using an equal gain combiner. To address this question we first attempt to determine if there is any way to distribute the given bandwidth and assign users so that total system SE is maximized. We add the restriction that all users should be able to transmit with the same data rates. After this, we address the question of how to allocate L antennas by dividing the serviced region into S sectors, each of them covered by $\approx L/S$ antennas. This is done by calculating average SE when users are randomly distributed within the region and considering the effects of antenna directivity on signal to noise ratio (SNR) at the receiver.

In responding to these questions, the rest of the paper is organized as follows: Section II describes the system, Section III studies bandwidth partitioning and Section IV studies cell sectoring. Overall results for system SE are presented in Section V, and Section VI presents some final remarks.

II. System description

The system consists of a single cell in which U users wish to transmit information to a base station. They are randomly distributed in a region, which is divided into S equal sectors, as shown in Fig. 1. Although users move, their distribution among the sectors varies very slowly with time. The base station knows at all times how many users there are

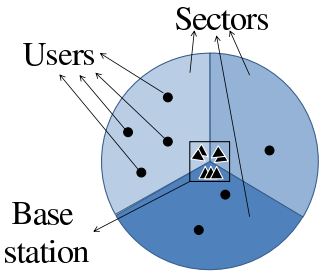

Fig. 1. Depiction of a system with $S = 3$ sectors, $U = 7$ users and $L = 7$ antennas.

in each sector. Sector s is covered by L_s directional antennas, where $s = 1, ..., S$, and $\sum_{s=1}^{S} L_s = L$. Different sectors may be covered by a different number of antennas. If $L/S > 1$, spatial diversity is also available in at least one sector.

The only available channel has bandwidth W. It suffers fast and frequency selective Rayleigh fading, thus preventing channel state estimation and tracking. The channel also suffers Additive White Gaussian Noise with power spectral density $N_0/2$. Long term statistics allows average received power estimation per user [17] and could be used to control received signal strength so that it is on average the same for all users in a sector. Thus, received energy per transmitted bit is E_b, the same for all users.

A multiuser MFSK system with joint non coherent detection may be employed because, as opposed to other digital modulations, its receiver does not require channel knowledge, unobtainable in a fast changing channel. Its innate (single user) low spectral efficiency is countered by using a multiuser system. It can be modeled by a concatenation of a noiseless U-users N-frequency multiple access channel [18] with N parallel fast fading frequency selective band limited channels, one per MFSK frequency. This system and its capacity have been studied in [19], [2], [20], for instance. It was shown in [20] that, in this situation, transmitter diversity does not improve transmission rate and that the best the receiver can do is to use an equal gain combiner [21] to obtain the required statistics.

III. Bandwidth partitioning

Considering that there is only one sector and all users within the cell share the whole bandwidth W simultaneously, overall SE for the sector, in [bits/s/Hz], is

$$\begin{aligned}\eta(N,U,L;E_b/N_0) &= \frac{1}{W}\frac{\mathcal{C}(N,U,L;E_b/N_0)}{\tau}\\ &= \frac{\mathcal{C}(N,U,L;E_b/N_0)}{N}\end{aligned} \tag{1}$$

where $\mathcal{C}(N,U,L;E_b/N_0)$ is the effective channel capacity as calculated in [20] and $\tau = N/W$ is symbol duration[1] . The value of $N = N^*$ that maximizes η depends on U, L and E_b/N_0, and increases with U. This maximum is called $\eta^*(U)$, in which arguments L and E_b/N_0 are omitted to simplify notation. On the other hand, there is a value of $U = U^*$ that maximizes η for a given N. This can lead to situations in which SE decreases with a small increase in the number of users because N^* is still the same, but $U > U^*$. Limiting the values of N to integer powers of 2, $\eta^*(U)$ for some values of L and E_b/N_0 is shown in Fig. 2, which exemplifies this behavior.

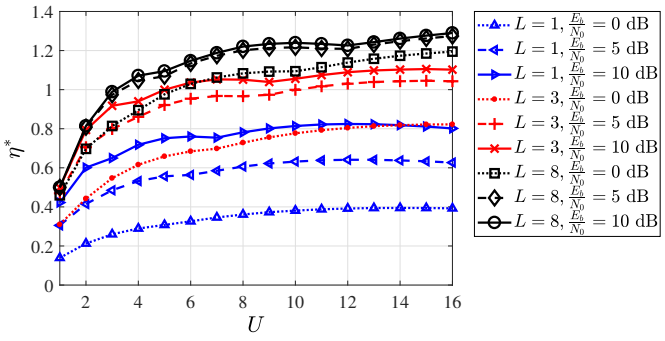

Fig. 2. Effects of U, L and E_b/N_0 on η^*. A local maximum occurs for instance at $U = 10$, $L = 8$ and $E_b/N_0 = 10$ dB, exemplifying a case in which a small increase in U decreases SE.

A possible strategy to attempt to increase SE would be to divide total bandwidth into D subchannels with bandwidths W_i, each with its own number of users U_i and a specific optimized value of N_i, $i = 1, 2, ..., D$. This combination can be described by the vectors $\mathbf{X} = [U_1 \;\; U_2 \cdots U_D]$ and $\mathbf{N} = [N_1 \;\; N_2 \cdots N_D]$. Obviously $D \leq U$ since otherwise there would be subchannels with no users. Overall SE would then be

$$\begin{aligned}\overline{\eta}(\mathbf{X}) &= \frac{1}{W}\sum_{i=1}^{D}\frac{\mathcal{C}(N_i,U_i,L;E_b/N_0)}{\tau_i}\\ &= \sum_{i=1}^{D} d_i \frac{\mathcal{C}(N_i,U_i,L;E_b/N_0)}{N_i}\\ &= \sum_{i=1}^{D} d_i \eta^*(U_i),\end{aligned} \tag{2}$$

where $d_i = W_i/W$,

$$N_i = \underset{N}{\operatorname{argmax}}\left\{\frac{\mathcal{C}(N,U_i,L;E_b/N_0)}{N}\right\}, \tag{3}$$

and

$$\eta^*(U_i) = \frac{\mathcal{C}(N_i,U_i,L;E_b/N_0)}{N_i} \tag{4}$$

is the spectral efficiency of subchannel $i = 1, 2, ..., D$.

To achieve such a scheme, the optimum values of $\mathbf{X}$, $\mathbf{N}$ and $\mathbf{D} = [d_1 \;\; d_2 \cdots d_D]$ should be found. By adding the restriction that all users must have the same single user rate, values of $\mathbf{N}$ and $\mathbf{D}$ are determined by $\mathbf{X}$. An exhaustive algorithm to find optimum value of $\mathbf{X}$ can be described as follows:

1) Generate a candidate user distribution $\mathbf{X}$ with elements $U_i > 0$, for $i = 1, 2, \cdots D$ and $\sum_{i=1}^{D} U_i = U$.
2) Find N_i as in (3).
3) Determine the values of d_i such that all users have the same single user rate, with $\sum_{i=1}^{D} d_i = 1$. Considering that all users must transmit with the same rate and that a user allocated to the i-th subchannel can transmit with rate $R = \mathcal{C}(N_i,U_i,L;E_b/N_0)/U_i$ bits per second, it is easily shown that
$$d_i = \frac{\dfrac{U_i}{\eta^*(U_i)}}{\displaystyle\sum_{j=1}^{D}\frac{U_j}{\eta^*(U_j)}} = \frac{RU_i}{W\eta^*(U_i)}. \tag{5}$$
These values have been calculated in the previous step.
4) Calculate candidate's $\overline{\eta}(\mathbf{X})$ according to (2).
5) Repeat the previous steps until all candidates have been evaluated.
6) The best candidate is the one that maximizes
$$\mathbf{X}^*(D) = \underset{\mathbf{X}}{\operatorname{argmax}}\left\{\overline{\eta}(\mathbf{X})\right\}. \tag{6}$$

[1]To this date there is no known closed expression relating N, U and L to η in this case. From [20], in general, as U increases, so does N that maximizes η and, for a given value of N, η is a concave function on U.

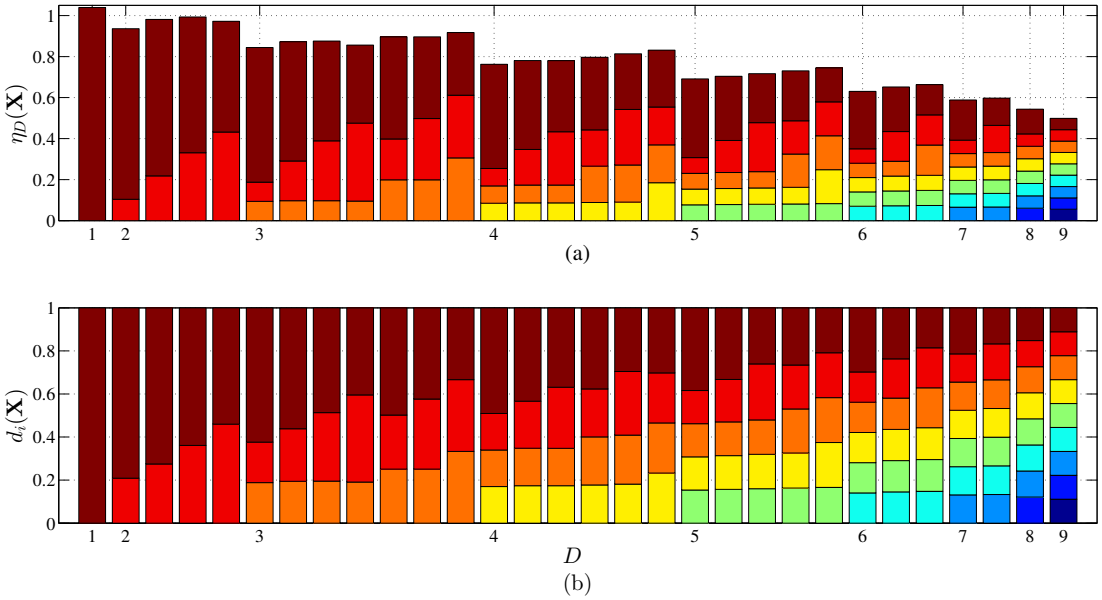

Fig. 3. Total spectral efficiency (a) and bandwidth division (b) for all candidate divisions $\mathbf{X}$ when $U = 9$, $L = 3$, and $E_b/N_0 = 10$ dB, excluding permutations. Each color represents a subchannel.

Although $\eta^*(U)$ is not a monotonically increasing function as shown in Fig. 2, it can be demonstrated that $D = 1$ is likely the best option. If $\eta^*(U) > \eta^*(U')$ for all $U' < U$, then $D = 1$ is clearly the best option. If there is $U' < U$ such that $\eta^*(U) < \eta^*(U')$ and the hypothesis that $D > 1$ maximizes $\overline{\eta}(\mathbf{X})$ over all possible values of D is true, then $\overline{\eta}(\mathbf{X}) = d_1\eta^*(U_1) + d_2\eta^*(U_2) + \cdots + d_D\eta^*(U_D)$. If it is indeed the best option, then

$$d_1\eta^*(U_1) + d_2\eta^*(U_2) > (d_1 + d_2)\eta^*(U_1 + U_2), \quad (7)$$

because otherwise joining the first two subchannels $(d_1 + d_2)$ and their respective number of users $(U_1 + U_2)$ must, by hypothesis, reduce overall SE. Employing the rightmost value of (5) for d_i and rearranging the terms leads to the following equivalent condition:

$$U_1 + U_2 > U_1\frac{\eta^*(U_1 + U_2)}{\eta^*(U_1)} + U_2\frac{\eta^*(U_1 + U_2)}{\eta^*(U_2)}. \quad (8)$$

Consider, without loss of generality, that $U_1 \geq U_2$. If U_2 is small: $\frac{\eta^*(U_1+U_2)}{\eta^*(U_1)} \approx 1$ because $U_1 \approx (U_1 + U_2)$; and $\frac{\eta^*(U_1+U_2)}{\eta^*(U_2)} > 1$. Then, most likely, condition (8) is not true. If $U_1 \approx U_2$, then, as illustrated in Fig. 6, most likely $\frac{\eta^*(U_1+U_2)}{\eta^*(U_1)} > 1$ and $\frac{\eta^*(U_1+U_2)}{\eta^*(U_2)} > 1$ and again (8) is not true. Thus, the new user distribution $\mathbf{X}' = [(U_1 + U_2)\ U_3 \cdots U_D]$ and optimized values $\mathbf{N}'$ and $\mathbf{D}'$ with $D-1$ elements result in higher SE than $\mathbf{X}, \mathbf{N}, \mathbf{D}$. The procedure repeats until $D = 1$. A sufficient but not required inequality for condition (8) to be true is that $\eta^*(U_i) > \eta^*(U_i + U_j)$ for all pairs $i, j = 1, ..., D$, which seems like a difficult imposition.

Fig. 3 shows some values of $\overline{\eta}$ for all candidates when $U = 9$, $D = 1, 2, ..., 9$, $L = 3$ and $E_b/N_0 = 10$ dB, a local minimum of η^* as a function of U, for some values of D. It is evident that sharing the whole available bandwidth is the best solution. When, for some other reason, it is necessary to divide the bandwidth, it is best to divide it as little and as equally as possible. The worst option is to perform frequency division multiple access, as indicated by the only case in which $D = 9$. Results for other values of U, L, and E_b/N_0 are similar, with the best case scenario always being the one with $D = 1$.

This analysis is also valid when $S > 1$: all users within a sector at a given time must share the whole bandwidth to maximize the sector's SE.

IV. Cell Sectoring

In the presence of $L > 1$ antennas at the receiver, two scenarios are possible to increase system SE:

- use all antennas to cover the whole region at the same time and use spatial diversity to improve system rate;

- divide the covered region into S sectors, where sector s is covered by L_s antennas, $s = 1, 2, ..., S$, $\sum_{i=1}^{S} L_s = L$.

In the first scenario, SE is given by (1). In the second scenario, there are three aspects to consider: antenna distribution, user distribution, and the effects of antenna directivity on SNR.

A. Antenna distribution

The most uniform way to distribute L antennas is to have b sectors covered by $L_s = a+1$ antennas each , $s = 1, 2, ..., b$, and $S - b$ sectors covered by $L_s = a$ antennas each for $s = b+1, b+2, ..., S$, with a and b nonnegative integers and $b < S$. The relationship between L and S can be written as

$$L = a \cdot S + b. \tag{9}$$

B. User distribution

There is no guarantee that users will be equally distributed among sectors. Let $\mathbf{Y} = [U_1 \quad U_2 \cdots U_S]$ be the number of users in each sector. If users are randomly distributed in the covered region with uniform distribution, then $U_i, i = 1, 2, ..., S$ are random variables with a binomial distribution and $\mathbf{Y}$ is a random vector with probability mass function given by

$$P(\mathbf{Y} = \mathbf{y}) = \frac{U!}{u_1! u_2! \cdots u_S!} \cdot \left(\frac{1}{S}\right)^U, \tag{10}$$

where $\mathbf{y} = [u_1 \quad u_2 \cdots u_S]$ is a realization of $\mathbf{Y}$.

C. Antennas and receiver chain

Fig. 4. shows a block diagram of the receiver chain at base station. As can be seen, it is composed of L RF receivers (with gain G, noise figure NF, and bandwidth W) cascaded to analog-to-digital converters (ADCs) whose output signals are sent to a multiuser detector (MUD). In addition, there is an antenna connected to the input of each RF receiver. We assume that if the number of sectors S is greater than or equal 2, then these antennas have an azimuth half-power beamwidth ϕ_a equal to $2\pi/S$ radians and their normalized power pattern $v(\theta, \phi)$ can be well approximated as the multiplication of an exponential function by an array factor of linear arrays, which describe the azimuth and elevation dependence, respectively, yielding

$$v(\theta, \phi) = \frac{\exp\left(-2.773\left(\frac{\phi}{\phi_a}\right)^2\right)}{M^2} \times \frac{\sin^2\left[\frac{ME(\cos(\theta)-\cos(\theta_m))}{2}\right]}{\sin^2\left[\frac{E(\cos(\theta)-\cos(\theta_m))}{2}\right]} \tag{11}$$

where M is the number of uniformly excited isotropic elements used to generate the array factor, E is the electrical distance between these elements, θ_m is the direction of the main lobe peak in the elevation plane, $0 \leq \theta \leq \pi$. The exponential function ensures that the pattern in the azimuth plane does not have sidelobes over the interval $-\pi/2 \leq \phi \leq \pi/2$. On the other hand, the array factor defines a main beam and sidelobes in the elevation plane. Patterns with such characteristics meet the sectoral antenna reference patterns presented in [22]. If $S = 1$, the antennas are omnidirectional, and the approximation for $v(\theta, \phi)$ reduces to only the array factor, which also complies with the recommendation given in [22]. In either case, increasing M or E leads to a narrower elevation half-power beamwidth (i.e., the directivity becomes higher), and for larger values of E, the number of sidelobes becomes greater.

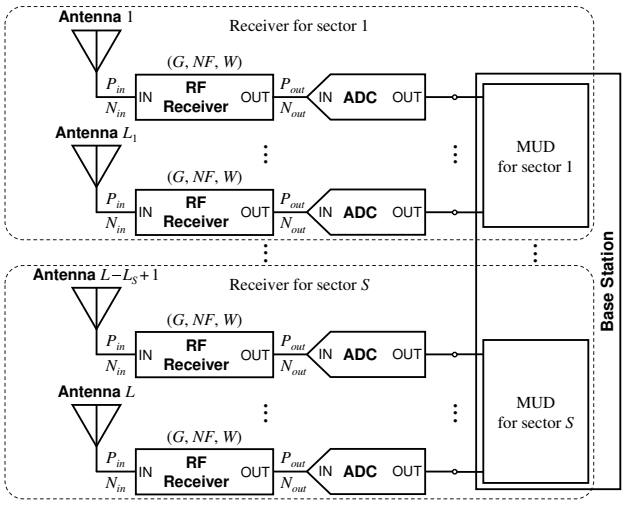

Fig. 4. Block diagram of a base station with L antennas and S sectors. Note that there are L radio frequency chains divided into S parallel receivers.

Fig. 5 shows examples of normalized patterns in elevation and azimuth planes computed with (11). Actually, they resemble the patterns of commercial

sector antennas used for cellular communications. It is worth noting that the assumption of the radiation pattern cut in elevation plane being independent of S is likely to be found in real scenarios because there are families of commercial sector antennas realized by linear arrays of printed dipoles or microstrip antennas, for example, showing this behavior [23].

In order to estimate the noise power N_{in} available at the terminals of the base station antennas, we first consider the background temperature T_{back} in the cell as that presented in [24] for the analysis of WCDMA base station capacity, i.e.,

$$T_{back}(\theta) = \begin{cases} \dfrac{1^\circ K}{(0.413\cos(\theta) + 0.013)} \\ \quad \text{if} \quad 0 \leq \theta < \pi/2; \\ 200^\circ K - 90^\circ K \cos(\theta) \\ \quad \text{if} \quad \pi/2 \leq \theta \leq \pi; \end{cases} \tag{12}$$

which is an absolute temperature in kelvin and the range $\pi/2 \leq \theta \leq \pi$ represents directions pointed toward the ground. The background temperature depends, among other factors, on frequency and on ground reflectivity, especially for $\theta \geq \pi/2$. Therefore, (12) expresses typical values that are representative at frequencies around 1 GHz.

Consequently, from (11) and (12), the brightness temperature T_b seen by the antennas may be evaluated as [25]

$$T_b = \frac{\int_{\phi=-\pi}^{\pi} \int_{\theta=0}^{\pi} T_{back}(\theta) v(\theta,\phi) \sin(\theta) d\theta d\phi}{\int_{\phi=-\pi}^{\pi} \int_{\theta=0}^{\pi} v(\theta,\phi) \sin(\theta) d\theta d\phi}. \tag{13}$$

Note that for the proposed scenario, the brightness temperature is independent of the number of sectors, since $v(\theta, \phi)$ is assumed separable, i.e., it is written as a product of functions of each variable θ and ϕ alone, and T_{back} is the same for all azimuth angles ϕ.

The antennas noise temperature T_a, in turn, is then [25]

$$T_a = k_i T_b + (1 - k_i) T_p \tag{14}$$

where k_i denotes the radiation efficiency $(0 \leq k_i \leq 1)$ and T_p indicates the physical temperature of the antennas in kelvin.

From (14), the noise power at the input of the RF receivers is computed as [25]

$$N_{in} = k T_a W \tag{15}$$

with k the Boltzmann constant. As a result, N_{in} does not change with S either and is a function of the antenna pattern in the elevation plane. Notice also that if the main lobe is tilted downward ($\theta_m > \pi/2$) to reduce interference into adjacent cells, for example, N_{in} is increased.

Since the available channel suffers fast and frequency selective Rayleigh fading where multipath propagation predominates, the signal power P_{in} at the input of the RF receivers is calculated in this paper using the antenna gain averaged over the solid angle in which $v(\theta, \phi) \geq 0.5$, leading to $P_{in} = c\,\overline{G}_S$, with $\overline{G}_S$ denoting the average gain as a function of S and c is a proportionality constant dependent on the transmitter and propagation channel characteristics. Thus, we can estimate the SNR (P_{out}/N_{out}) at the input of the ADCs through

$$\frac{P_{out}}{N_{out}} = \frac{c\,\overline{G}_S}{k(T_a + T_0(NF - 1))W} \tag{16}$$

in which $T_0 = 290\,\text{K}$ is the standard noise temperature.

Therefore, if the number of sectors changes, but both the radiation pattern cut in elevation plane and the transmit power limitation for users remain the same regardless of S, then the variation of the SNR is equal to that of $\overline{G}_S$, since T_a is not a function of S, as explained previously. Assuming that the transmit power limitation for users is the same regardless of the number of sectors, the increment Δ_S in P_{out}/N_{out} and consequently in E_b/N_0 caused by using S sectors instead of one is then

$$\Delta_S = \frac{\overline{G}_S}{\overline{G}_1}. \tag{17}$$

Numerical values for $\overline{G}_S$ and Δ_S are summarized in Table I considering $M = 8$, $M = 16$ and $S = 1$ to 8. As seen, when the number of sectors is increased from 1 (omnidirectional antenna) to 8 in the configurations analyzed, $\overline{G}_S$ as well as the SNR at the input of the ADCs will be about 8 dB higher.

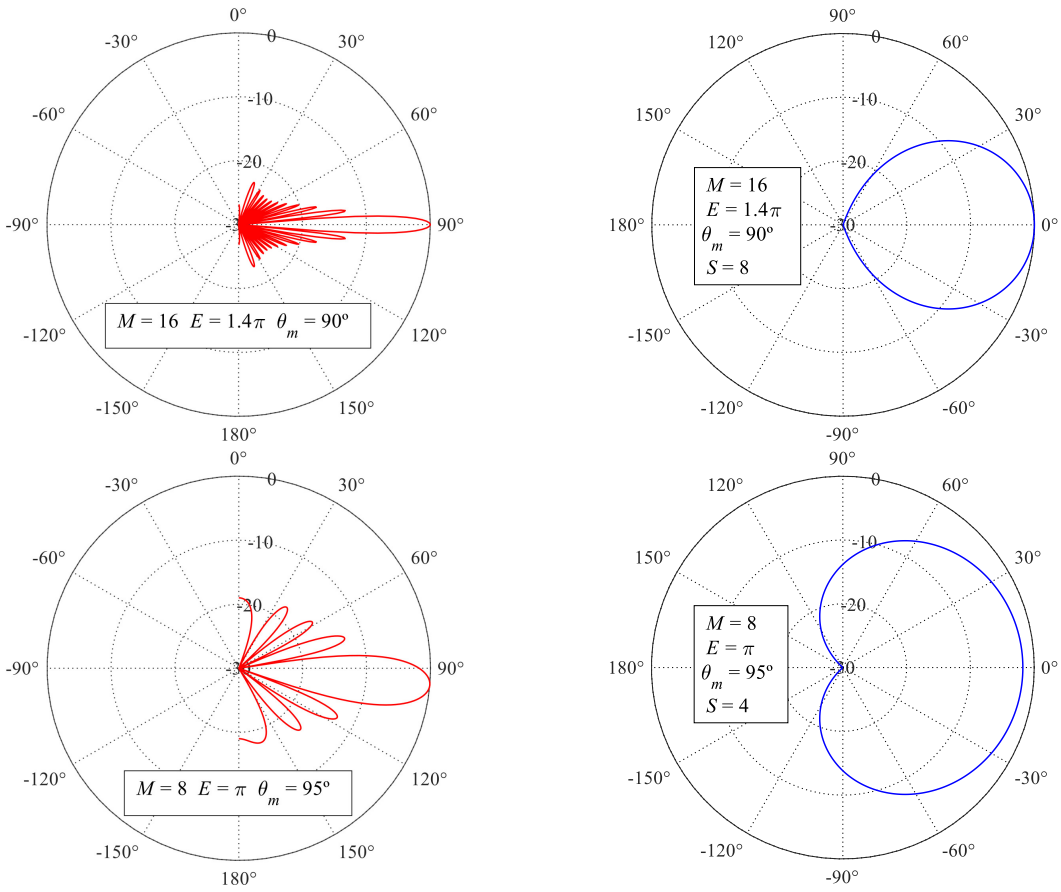

Fig. 5. Normalized power patterns in dB. Left column: elevation patterns, Right column: azimuth patterns

D. System spectral efficiency

Since sectors can have a different number of antennas, system's average total SE is given by

$$\eta_S = \sum_{\mathbf{y}\in\Gamma(\mathbf{y})} P(\mathbf{Y}=\mathbf{y}) \cdot \left[\sum_{s=1}^{S} \frac{\mathcal{C}\left(N_s^*, u_s, L_s; \frac{E_b}{N_0}\cdot\Delta_S\right)}{N_s^*} \right] \tag{18}$$

where $\Gamma(\mathbf{y})$ is the set of all possible values of $\mathbf{y}$. When $S > 1$ and L/S is an integer, all sectors are covered by the same number of antennas and (18) simplifies to:

$$\eta_S = S \sum_{u=0}^{U} \binom{U}{u} \left(\frac{1}{S^u}\right) \left(\frac{S-1}{S}\right)^{(U-u)} \times \eta\left(N^*, u, \frac{L}{S}; \frac{E_b}{N_0}\cdot\Delta_S\right). \tag{19}$$

V. Results and Analysis

To compare systems with different E_b/N_0 due to antenna directivity, a reference value of $(E_b/N_0)_R$ is established as the value that would be seen by the receiver when $S = 1$. For example, given that $\Delta_2 = 2.31$ dB, a signal received with $(E_b/N_0)_R = 5$ dB results in $E_b/N_0 = 7.31$ dB when $S = 2$. The following results are expressed as a function of this reference value. The case in which $S = 1$ is also the benchmark case in which only MIMO (in this case, multiple output) is used.

Fig. 6 presents results for η_S for $S = 1, 2, ..., 8$, $L = 8$ and $(E_b/N_0)_R = 5$ dB as a function of U. In this case, it is always better to have $S = L$ sectors, each covered by a single antenna, even if at times a sector might have no users. Gain in η_S due to a higher value of S increases as the number of users increases, but incremental gain decreases.

SNR seems to have no effect on the best choice of S as seen in Fig. 7. It also shows that for $S = 1$, an increase in E_b/N_0 is unable to make η_S reach values achievable by higher values of S, while for high S an increase of less than 2 dB makes up for the loss in η_S caused by using less sectors. Required increase to reach the same SE reduces for higher S.

TABLE I
VALUES OF $\overline{G}_S$ (IN DBI) AND Δ_S (IN DB) FOR COMBINATIONS OF SOME TYPICAL VALUES OF E (IN RADIANS), k_i, M, TWO TILTING ANGLES AND S RANGING FROM 1 TO 8.

S	$\theta_m = 90°$, $E = \pi$, $k_i = 0.85$				$\theta_m = 95°$, $E = 1.4\pi$, $k_i = 0.85$				$\theta_m = 95°$, $E = \pi$, $k_i = 0.85$			
	$M = 8$		$M = 16$		$M = 8$		$M = 16$		$M = 8$		$M = 16$	
	$\overline{G}_S$	Δ_S	$\overline{G}_S$	Δ_S	$\overline{G}_S$	Δ_S	$\overline{G}_S$	Δ_S	$\overline{G}_S$	Δ_S	$\overline{G}_S$	Δ_S
1	7.45	0	10.45	0	8.78	0	11.85	0	7.44	0	10.45	0
2	9.75	2.3	12.76	2.31	11.09	2.31	14.15	2.31	9.75	2.31	12.76	2.31
3	11.43	3.98	14.44	3.99	12.77	3.99	15.84	3.99	11.43	3.99	14.44	3.99
4	12.67	5.22	15.68	5.23	14.02	5.24	17.08	5.23	12.67	5.23	15.68	5.23
5	13.65	6.2	16.65	6.2	14.99	6.21	18.05	6.2	13.64	6.2	16.65	6.2
6	14.44	6.99	17.45	7.00	15.78	7.00	18.84	7.00	14.44	7.00	17.45	7.00
7	15.10	7.65	18.11	7.66	16.45	7.67	19.51	7.66	15.10	7.66	18.11	7.66
8	15.68	8.23	18.69	8.24	17.03	8.25	20.09	8.24	15.68	8.24	18.69	8.24

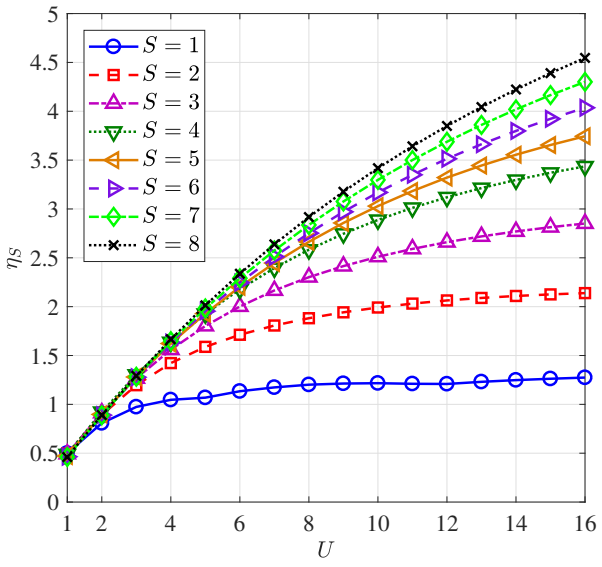

Fig. 6. Spectral efficiency as a function of U for some values of S, $L = 8$ and $(E_b/N_0)_R = 5$ dB.

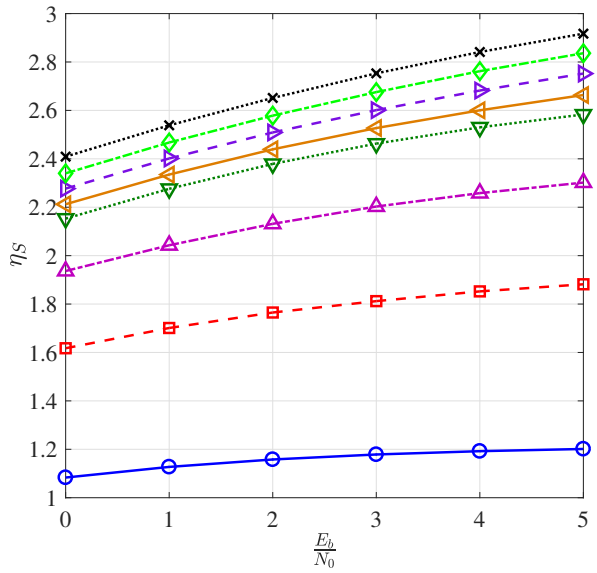

Fig. 7. Spectral efficiency as a function of $(E_b/N_0)_R$ (in dB) for some values of S, $L = 8$ and $U = 8$. Labels are the same as in Fig. 6 .

However, this increase is not due to Δ_S by itself. This is illustrated when comparing the cases in which $S = 7$ and $S = 8$. An increase of around 1 dB is necessary, while $\Delta_8 - \Delta_7 = 0.54$ dB. The trade-off between number of sectors and E_b/N_0 may be considered when implementing a system, because the additional energy requirement at the transmitters might relieve processing energy requirement at the receiver.

Fixing $U = 20$, $(E_b/N_0)_R = 5$ dB and making $L = 8, 16, 24, 32$ leads to Fig. 8. For $S = 8$, each sector is covered respectively by 1 to 4 antennas. It is clear that most of the diversity gain is obtained when L is small. Thus, it is better to create a new sector than to cover the same sector with more antennas, if it is already covered by more than one, assuming that antennas with the appropriate design are available. The reason for this behavior is that, when increasing the number of sectors from S to $S + 1$, SNR at the ADC is increased by $\Delta_{S+1} - \Delta_S$ and causes an increase in SE higher than a gain in the number of antennas from L to $L + 1$. Moreover, if there are S sectors to begin with, $L = S$ antennas would be required to add one antenna to each subsector. The better alternative is to use $2S$ sectors instead.

Combining the results from Figs. 7 to 8, it is

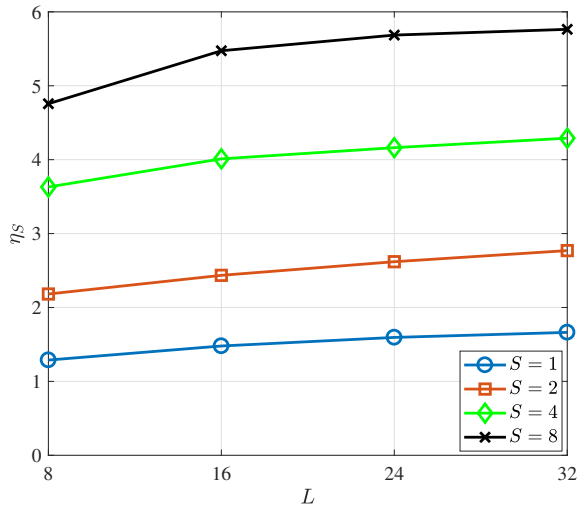

Fig. 8. Spectral efficiency as a function of L, $U = 20$, $(E_b/N_0)_R = 5$ dB.

evident that a higher value of S allows values of SE that are unachievable by the benchmark case in which $S = 1$ even whit an increase on U or $(E_b/N_0)_R$. Furthermore, it is possible to, given an initial SE, increase S, decrease required $(E_b/N_0)_R$ and still maintain same initial SE. Lowering required $(E_b/N_0)_R$ directly impacts on required transmitted power, thus making the system more energy efficient.

These results may be explained by analyzing the effects of S on (19). First, the number of sectors multiplies the summation. This by itself increases SE. However, the gain linear improvement in SE because of other effects of S on SE. The effect of user distribution among sectors may be analyzed considering that the probability of a user being in a specific sector is $1/S$. As a consequence, the number of users per sector is a binomial random variable with average U/S that decreases with an increase in S. This is not harmful for η_S because $\eta^*(U)$ does not change much with U if $U > U'$, where U' depends on L_s and E_b/N_0 as illustrated in Fig. 6. For example, $\eta^*(16) < 2\eta^*(2)$ for all cases in Fig. 2. In fact, the number of sectors could take into account the value of U', aiming to make $U/S = U'$. Fig. 6 shows this criterion: fixing U and considering $U' = 2$, η_S is similar for all cases when $U/S < 2$, regardless of S.

The number of sectors plays two roles in $\eta^*(u)$: it improves E_b/N_0 due to higher antenna directivity as shown in Table I, thus increasing SE; it decreases L/S, decreasing SE. Table II shows that the effect of S on $\eta\left(N^*, u, \frac{L}{S}; \frac{E_b}{N_0} \cdot \Delta_S\right)$ by itself is a decrease of around 20% when S changes from 1 to 8, $U = 5$ and $(E_b/N_0)_R = 5$ dB. Thus, the overall effect of an increase in S is an increase in SE because the decrease in $\eta^*(u)$ is no match to the linear increase on the number of sectors and better user distribution.

TABLE II
VALUES OF $\eta\left(N^*, 5, \frac{L}{S}; \frac{E_b}{N_0} \cdot \Delta_S\right)$ IN [BITS/S/HZ] WHEN $(E_b/N_0)_R = 5$ DB.

S	L			
	8	16	24	32
1	1.068	1.194	1.258	1.303
2	1.012	1.084	1.163	1.213
3	0.944	1.025	1.055	1.096
4	0.833	0.974	1.010	1.029

These results support the claim that, in this particular case, it is better to divide a cell in $S = L$ sectors than to use diversity, resulting in $L_s = 1$. In case S is unfeasible for some other reason, S should be as large as possible.

VI. CONCLUSIONS

This paper studies some strategies to improve system spectral efficiency of a multiuser MFSK system that uses a fast and frequency selective fading channel. Considered strategies were bandwidth partitioning and cell sectoring. There are two main results. The first major result is that bandwidth partitioning does not improve spectral efficiency. If required by some other reason, it should be divided into the least amount of partitions. Also, partitioning should be as uniform as possible. The second major result is that, in this case, sectoring is better than diversity, even at the cost of losing diversity. Gains due to sectoring depend on the number of users, available antennas/receiver chains, and signal to noise ratio. Sectoring is better because sectors improve user distribution and overall spectral efficiency is the sum of each sector's average efficiency.

These results may impact system design because total data rate and energy consumption aspects are affected by them. Clearly, sectoring allows the system to reach spectral efficiencies unachievable by systems that employ only MIMO. Also, these higher spectral efficiencies may be achieved by significantly lowering requirements for received, and

consequently transmitted, power, thus increasing energy efficiency(EE). Both of these efficiencies are key factors in 5G [26] and beyond.

Future research may deal with how sectoring affects systems with multiple cells and the combination of these results with other strategies to improve spectral efficiency. Also, it may be of interest to perform this comparison to other channel models. In particular, the mmWave band considered for vehicular communications [27] allows usage of a high number of antennas on a limited circuit area due to the higher frequency but, although it suffers fast and frequency selective fading, its statistics are not well modeled by the Rayleigh distribution [8], [9], and background noise models are not available yet.

REFERENCES

[1] D. J. Goodman, P. S. Henry, and V. K. Prabhu, "Frequency-hopped multilevel fsk for mobile radio," *Bell Syst. Tech. J.*, vol. 59, no. 7, pp. 1257–1275, Sep. 1980. doi: 10.1002/j.1538-7305.1980.tb03360.x.

[2] M. Sharma and J. Portugheis, "On the sum capacity of a t-user n-frequency multiple access channel with noise," *European Trans. on Telecommun.*, vol. 21, no. 1, pp. 23–29, 2010. doi: 10.1002/ett.1351.

[3] J. Winters, "On the capacity of radio communication systems with diversity in a rayleigh fading environment," *IEEE J. on Sel. Areas in Commun.*, vol. 5, no. 5, pp. 871–878, Jun. 1987. doi: 10.1109/JSAC.1987.1146600.

[4] A. Goldsmith, S. Jafar, N. Jindal, and S. Vishwanath, "Capacity limits of mimo channels," *IEEE J. on Sel. Areas in Commun.*, vol. 21, no. 5, pp. 684–702, Jun. 2003. doi: 10.1109/JSAC.2003.810294.

[5] S. Alamouti, "A simple transmit diversity technique for wireless communications," *IEEE J. on Sel. Areas in Commun.*, vol. 16, no. 8, pp. 1451–1458, Oct. 1998. doi: 10.1109/49.730453.

[6] A. A. Nasir, H. Mehrpouyan, D. Matolak, and S. Durrani, "Non-coherent FSK: An attractive modulation set for millimeter-wave communications," in *2016 IEEE Wireless Commun. and Netw. Conf.*, pp. 1–7. IEEE, Apr. 2016. doi: 10.1109/wcnc.2016.7565093.

[7] E. G. Larsson, O. Edfors, F. Tufvesson, and T. L. Marzetta, "Massive MIMO for next generation wireless systems," *IEEE Commun. Mag.*, vol. 52, no. 2, pp. 186–195, Feb. 2014. doi: 10.1109/mcom.2014.6736761.

[8] C. Lv, J.-C. Lin, and Z. Yang, "Channel prediction for millimeter wave MIMO-OFDM communications in rapidly time-varying frequency-selective fading channels," *IEEE Access*, vol. 7, pp. 15 183–15 195, 2019. doi: 10.1109/access.2019.2893619.

[9] J. Huang, C.-X. Wang, H. Chang, J. Sun, and X. Gao, "Multi-frequency multi-scenario millimeter wave MIMO channel measurements and modeling for b5g wireless communication systems," *IEEE J. on Sel. Areas in Commun.*, vol. 38, no. 9, pp. 2010–2025, Sep. 2020. doi: 10.1109/jsac.2020.3000839.

[10] J. Lorca, M. Hunukumbure, and Y. Wang, "On overcoming the impact of doppler spectrum in millimeter-wave V2I communications," in *2017 IEEE Globecom Workshops*. IEEE, Dec. 2017. doi: 10.1109/glocomw.2017.8269039.

[11] B. D. V. Veen and K. M. Buckley, "Beamforming: a versatile approach to spatial filtering," *IEEE ASSP Mag.*, vol. 5, no. 2, pp. 4–24, Apr. 1988. doi: 10.1109/53.665.

[12] S. Chinnadurai, P. Selvaprabhu, Y. Jeong, A. L. Sarker, H. Hai, W. Duan, and M. H. Lee, "User clustering and robust beamforming design in multicell MIMO-NOMA system for 5g communications," *AEU - Int. J. of Electron. and Commun.*, vol. 78, pp. 181–191, Aug. 2017. doi: 10.1016/j.aeue.2017.05.021.

[13] S. Zhou, M. Zhao, X. Xu, J. Wang, and Y. Yao, "Distributed wireless communication system: a new architecture for future public wireless access," *IEEE Commun. Mag.*, vol. 41, no. 3, pp. 108–113, Mar. 2003. doi: 10.1109/mcom.2003.1186553.

[14] V. Jungnickel, K. Manolakis, W. Zirwas, B. Panzner, V. Braun, M. Lossow, M. Sternad, R. Apelfrojd, and T. Svensson, "The role of small cells, coordinated multipoint, and massive MIMO in 5g," *IEEE Commun. Mag.*, vol. 52, no. 5, pp. 44–51, May 2014. doi: 10.1109/mcom.2014.6815892.

[15] M. Mozaffari, W. Saad, M. Bennis, and M. Debbah, "Drone small cells in the clouds: Design, Deployment and Performance Analysis," in *2015 IEEE Globecom*. IEEE, pp. 1–6, Dec. 2015. doi: 10.1109/glocom.2015.7417609.

[16] X. Li, C. He, D. Feng, C. Guo, and J. Zhang, "Power allocation criteria for distributed antenna systems with D2D communication," *AEU - Int. J. of Electron. and Commun.*, vol. 93, pp. 109–115, Sep. 2018. doi: 10.1016/j.aeue.2018.05.036.

[17] M. Sharma, "Data-aided power estimation for a multiuser non coherent MFSK fast rayleigh fading system," in *2017 SBMO/IEEE MTT-S Int. Microw. and Optoelectronics Conf. (IMOC)*. IEEE, Aug. 2017. doi: 10.1109/imoc.2017.8121143.

[18] S.-C. Chang and J. Wolf, "On the t-user m-frequency noiseless multiple-access channel with and without intensity information," *IEEE Trans. on Inf. Theory*, vol. 27, no. 1, pp. 41–48, Jan. 1981. doi: 10.1109/TIT.1981.1056304.

[19] O.-C. Yue, "Maximum likelihood combining for noncoherent and differentially coherent frequency-hopping multiple-access systems," *IEEE Trans. on Inf. Theory*, vol. 28, no. 4, pp. 631–639, Jul. 1982. doi: 10.1109/TIT.1982.1056532.

[20] M. Sharma, "Effects of diversity on the sum rate of a multiuser m-FSK system over fast rayleigh fading channel," in *Anais de XXXV Simpósio Brasileiro de Telecomunicações e Processamento de Sinais*. Sociedade Brasileira de Telecomunicações, 2017. doi: 10.14209/sbrt.2017.13.

[21] N. Yee, J.-P. Linnartz, and G. Fettweis, "Multi-carrier cdma in indoor wireless radio networks," *IEICE Trans. on Commun.*, vol. 77, no. 7, pp. 900–904, 1994.

[22] *ITU-R F.1336-5 Reference radiation patterns of omnidirectional, sectoral and other antennas for the fixed and mobile services for use in sharing studies in the frequency range from 400 MHz to about 70 GHz*, Int. Telecommunications Union Std., 2019.

[23] Z. N. Chen and K.-M. Luk, (Eds.), *Antennas for Base Stations in Wireless Communications*. McGraw Hill, 2009. ISBN 0071612882.

[24] K. Steinhauser, "Influence of antenna noise temperature and downtilt on wcdma base station capacity," in *2009 3rd European Conf. on Antennas and Propag.*, 2009, pp. 3307–3311.

[25] D. M. Pozar, *Microwave engineering*. John Wiley & Sons, 2011.

[26] N. Alliance, "5g white paper," *Next generation mobile networks, white paper*, vol. 1, 2015.

[27] F. J. Martin-Vega, M. C. Aguayo-Torres, G. Gomez, J. T. Entrambasaguas, and T. Q. Duong, "Key technologies, modeling approaches, and challenges for millimeter-wave vehicular communications," *IEEE Commun. Mag.*, vol. 56, no. 10, pp. 28–35, Oct. 2018. doi: 10.1109/mcom.2018.1800109.

Manish Sharma received his Electrical Engineering degree in 2003, his Master's degree in Electrical Engineering in 2006 and his Doctorate in Electrical Engineering in 2010, all from the University of Campinas (Unicamp). Since 2009 he is a professor at the Aeronautics Institute of Technology. His main research interests are multiuser communication systems and channel coding.

Daniel Basso Ferreira received the B.S. degree (summa cum laude) in electronics engineering and the M.S. and D.S. degrees in electronics and computer engineering from the Aeronautics Institute of Technology, Sao Jose dos Campos, Brazil, in 2009, 2011, and 2017, respectively. He is currently an Assistant Professor at the Department of Microwaves and Optoelectronics, Aeronautics Institute of Technology, Sao Jose dos Campos, Brazil, and a member of the Laboratory of Antennas and Propagation (LAP/ITA). His research work is mainly focused on microstrip antennas mounted on curved surfaces, frequency-independent antennas, and antenna arrays.